

U K /99-14
Oct. 1999

Parton Degrees of Freedom from the Path-Integral Formalism

K eh-Fei Liu

N ational C enter for T heoretical S ciences, P . O . B ox 2-131, H sinchu, T aiwan 300
and

D ept. of P hysics and A stronom y, Univ. of K entucky, L exington, K Y 40506

A bstract

We formulate the hadronic tensor W of deep inelastic scattering in the path-integral formalism. It is found that there are 3 gauge invariant and topologically distinct contributions which correspond to the valence, cloud and sea partons. The phenomenological consequences of this classification in terms of the small x behavior, Gottfried sum rule violation, and evolution are emphasized. The operator product expansion is carried out in the path-integral formalism. The operator rescaling and mixing reveal that the cloud and anticloud partons evolve the same way as the valence, not the sea in the disconnected insertion.

PACS numbers: 11.15.H a, 13.60.H b, 13.60.-r

1 Introduction

In the last decade, the surprising results of a small quark spin content (a vector-singlet g_a^0) [1] and the discovery that $u \neq d$ in the nucleon [2] from deep inelastic scattering have focused people's attention on the interplay between the parton model at high energies and the hadronic structure at low energies. The connection is often made through the operator product expansion which relates the sum rules of parton distribution functions with the forward matrix elements. The latter can be obtained from low energy experiments.

In the parton model, the dynamical quark degrees of freedom are taken to be the valence and the sea. Whereas, in the hadronic models, the degrees of freedom involve the valence and the meson cloud. The classification of these dynamical degrees of freedom in deep inelastic scattering has been made in the path integral formalism [3, 4] recently. Their relations to the meson cloud in the hadronic models for hadrons near the rest frame and chirality symmetry have been clarified and extensively explored in the context of hadronic models in terms of the form factors, hadron masses, and matrix elements, i.e. low-energy quantities which are observables in the two- and three-point functions. In addition, it is shown that when the cloud and sea quarks are eliminated in a valence QCD theory, the valence quark picture with $SU(6)$ symmetry emerges. In this paper, we shall explore the phenomenological consequences of the parton degrees of freedom. In particular, we shall show that the small x behavior of the cloud and anti-cloud is different from that of the sea. We will also show how to carry out the operator product expansion in the path-integral formalism. From this expansion and operator rescaling and mixing, we reveal that the cloud evolves like the valence not the sea. As a consequence, the parton evolution equations need to accommodate this cloud degree of freedom explicitly.

2 Path-Integral Formalism

The deep inelastic scattering of a muon on a nucleon involves the hadronic tensor which, being an inclusive reaction, involves all intermediate states

It has been shown [3, 4] that the hadronic tensor $W_{\mu\nu}(q^2)$ can be obtained from the Euclidean path-integral formalism where the various parton dynamical degrees of freedom are readily and explicitly revealed. In this case, one considers the ratio of the four-point function $\frac{2E_p V}{2M_N} h_{O_N}(t) \frac{d^3 x}{2} e^{iq \cdot x} J(x; t_2) J(0; t_1) O_N(0) i$ and the two-point function $h_{O_N}(t - (t_2 - t_1)) O_N(0) i$, where $O_N(t)$ is an interpolation field for the nucleon with momentum p at Euclidean time t .

As both $t - t_2 \gg 1 = M_N$ and $t_1 \gg 1 = M_N$, where M_N is the mass gap between the nucleon and the next excitation (i. e. the threshold of a nucleon and a pion in the p-wave), the intermediate state contributions will be dominated by the nucleon with the Euclidean propagator $e^{M_N(t(t_2-t_1))}$. Hence, this defines the quantity

$$\tilde{W}(q^2; \tau) = \frac{1}{2M_N} \sum_n (2\pi)^2 \delta^3(p_n - p + q) \bar{h}^N(t(0)) h^N(t(0)) N \text{spin ave.} e^{(E_n - E_N)} : \quad (2)$$

where $\tau = t_2 - t_1$. To go back to the delta function $(E_n - E_N + i\epsilon)$ in Eq. (1), one needs to carry out the inverse Laplace transform [5, 3]

$$W(q^2; \tau) = \frac{1}{i} \int_{-c-i\infty}^{c+i\infty} dz e^{-z\tau} \tilde{W}(q^2; z); \quad (3)$$

with $c > 0$. This is basically doing the anti-Wick rotation back to the Minkowski space.

In the Euclidean path-integral formulation of $\tilde{W}(q^2; \tau)$ in Eq. (2), contributions to the four-point function can be classified according to different topologies of the quark paths between the source and the sink of the proton. They represent different ways the fields in the currents J and \bar{J} contract with those in the nucleon interpolation operator O_N . Fig. 1(a) and 1(b) represent connected insertions (C.I.) of the currents. Here the quark fields from the interpolators O_N contract with the currents such that the quark lines flow continuously from $t=0$ to $t=t$. Fig. 1(c), on the other hand, represents a disconnected insertion (D.I.) where the quark fields from J and \bar{J} self-contract and are hence disconnected from the quark paths between the proton source and sink. Here, "disconnected" refers only to the quark lines. Of course, quarks dive in the background of the gauge field and all quark paths are ultimately connected through the gluon field.

Fig. 1 represents the contributions of the class of "handbag" diagrams where the two currents are hooked on the same quark line. These contain leading twist contributions in deep inelastic scattering. Other contractions involving the two currents hooking on different quark lines involve only higher twist operators and thus will be suppressed in the Bjorken limit [4]. They are shown in Fig. 2. We will neglect these "cat's ears" diagrams from now on.

In the deep inelastic limit, the Bjorken scaling implies that the current product (or commutator) is dominated by the light-cone singularity of a free-field theory, i. e. $1=x^2$ where $x^2 \equiv 0 (1=Q^2)$. Among the three-exact diagrams in Fig. 1, Fig. 1(a)/1(b) involves only a quark/antiquark propagator between the currents; whereas, Fig. 1(c) has both quark and antiquark propagators. Hence, there are two distinct classes of diagrams where the antiquarks contribute. One comes from the D.I.; the other comes from the C.I.. It is usually assumed that connected insertions involve only "valence" quarks which are responsible for the baryon number. This is obviously not true.

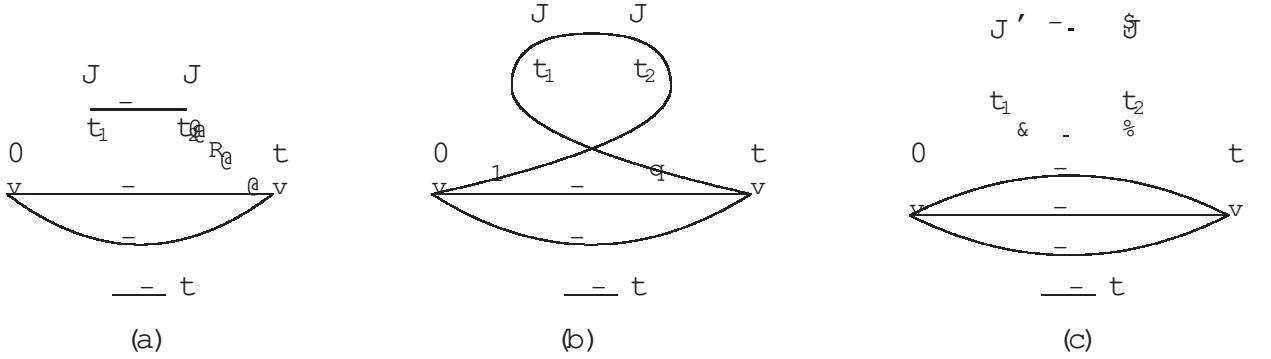


Figure 1: Quark skeleton diagrams in the Euclidean path integral formalism for evaluating W from the four-point function defined in Eq. (2). These include the lowest twist contributions to W . (a) and (b) are connected insertions and (c) is a disconnected insertion.

There are also quark-antiquark pairs in the C. I. To define the quark distribution functions more precisely, we shall call the antiquark distribution from the D. I. (which are connected to the "valence" quark propagators and other quark loops through gluons) the "sea" quark. We shall refer to the antiquark in the backward time going quark propagator between t_1 and t_2 in Fig. 1(b) as the "cloud" antiquark. On the other hand, the quark in the time forward propagator between t_2 and t_1 in Fig. 1(a) includes both the valence and the cloud quarks. This is because a quark propagator from $t = 0$ to $t = t$ ($t > 0$) involves both the time forward and backward zigzag motions so that one cannot tell if the quark propagator between t_2 and t_1 is due to the valence or the cloud. All one knows is that it is a quark propagator. In other words, one needs to consider cloud quarks in addition to the valence in order to account for the production of cloud quark-antiquark pairs in a connected fashion (Fig. 1(a)); whereas, the pair production in a disconnected fashion is in Fig. 1(c).

We should stress that this separation into three topologically distinct classes of path-integral diagrams is gauge invariant as far as the quark lines in Fig. 1 are concerned (all the quark propagators are sewed together in a trace over color). In a perturbative illustration of the distinction between Fig. 1(b) and Fig. 1(c), one may consider the time-ordered perturbation where Fig. 1(c) represents the vacuum polarization contribution as a disconnected insertion in a direct diagram. The corresponding exchange diagram where the quark in the loop in Fig. 1(c) is exchanged with

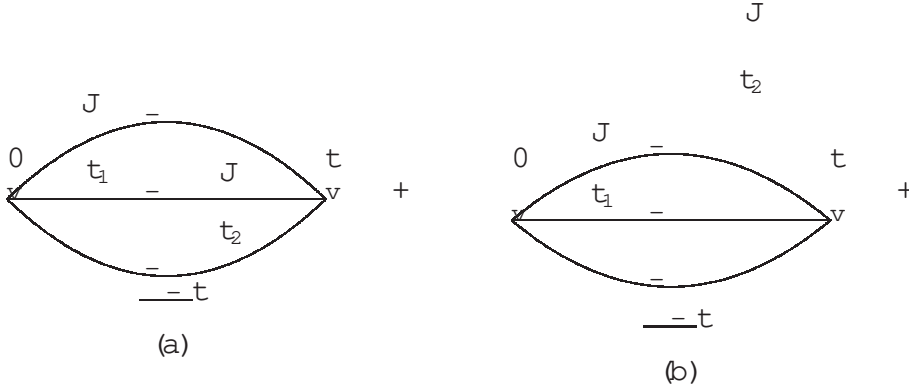


Figure 2: Quark skeleton diagrams similar to those in Fig. 1, except that the two current insertions are on different quark lines. They give higher twist contributions to W .

one in the ‘valence’ will lead to a connected insertion which falls in the class of Fig. 1(b) [3, 6]. However, the separation depends on the momentum frame of the nucleon, although the sum which corresponds to the full physical W (q^2 ;) does not. For example, when the quark/antiquark propagator between the currents is either from the nucleon interpolation field or pair-produced before the current J at t_1 , i.e. it is pre-existing in the wavefunction, then it is not suppressed in the large momentum frame. Whereas, if it is pair-produced by the current J , then it is suppressed by p_j^2 where p_j is the momentum of the nucleon. This has been known since current algebra sum rules were studied at large p_j [7].

Since the parton model acquires its natural interpretation in the large momentum frame of the nucleon, i.e. $p_j \gg p$, the parton distribution is then defined via $W_2(Q^2;) = \int \frac{dx}{x} e_i^2(q_i(x; Q^2) + \bar{q}_i(x; Q^2))$ in the large momentum frame. Here x is the Bjorken scaling variable $x = Q^2/2m$. Given the specific time-ordering in Fig. 1, Fig. 1(a)/1(b) involves only a quark/antiquark propagator between the currents; whereas, Fig. 1(c) has both quark and antiquark propagators. Consequently, the parton density for the u and d antiquarks come from two sources.

$$\bar{q}(x) = \bar{q}_c(x) + \bar{q}_s(x); \quad (4)$$

where $\bar{q}_c(x)$ is the anticloud parton distribution from the C. I. in Fig. 1(b) and $\bar{q}_s(x)$ denotes the antisea parton distribution from the D. I. in Fig. 1(c). The strange and charm quarks would only contribute in the D. I. in Fig. 1(c). Similarly, the u and d

partons have 2 sources, i.e.

$$q(x) = q_{v+c}(x) + q_s(x); \quad (5)$$

where $q_{v+c}(x)$ denotes the valence and cloud partons and $q_s(x)$ denotes the sea parton and they are from Fig. 1(a) and Fig. 1(c) respectively.

3 Phenomenological consequences

After the dynamical parton degrees of freedom are classified as valence, cloud, and sea via the path-integral diagrams in Fig. 1, one may question why we need to separate the cloud from the sea. After all, both the cloud and sea are pair-produced and one can simply call them connected sea and disconnected sea. In the following, we shall show that it is necessary to separate one from the other because they have different small x behaviors and, furthermore, they evolve differently.

3.1 Small x behavior

It is shown by Brodsky and Schmidt [8] that the structure functions can be separated into intrinsic and extrinsic parts via the empty target consideration. Furthermore, they show that neither the Pomeron nor the leading Reggeon contribution is present in the intrinsic part based on the charge conjugation and crossing symmetry considerations. Consequently, the intrinsic distribution has an $x^{1/2}$ behavior for small x and vanishes for $x \rightarrow 0$. This is in contrast to the x^1 behavior of the extrinsic distribution. Since the extrinsic part is defined as the contribution in DIS when the electric charges of the valence quarks are turned off, it is clear that neither Fig. 1(a) nor Fig. 1(b) can contribute as the quark/antiquark there originates from the valence interpolation field and does not carry electric charge by definition. It can only be identified with the sea distribution in Fig. 1(c). In this case, the virtual photon can couple to the quarks in the fermion loop which carry electric charge and the interaction between the loop and the valence quarks from the nucleon can be mediated by the gluons. From this identification, we conclude that the parton distributions of q_{v+c} and q_s have the $x^{1/2}$ form and q_v and q_s have the x^1 form at small x .

3.2 Origin of Gottfried sum rule violation

The EMC experiments of the F_2 structure functions of the proton and deuteron [2] reveal that the Gottfried sum rule

$$S_G = \int_0^1 dx \frac{F_2^p(x) - F_2^n(x)}{x} = \frac{1}{3}; \quad (6)$$

is violated due to fact that $u \neq d$ in the proton. This is verified in the Drell-Yan experiment E866/NuSea [9]. It has been shown [3] that the sea partons in Fig. 1(c) cannot give rise to a different u and d . It is noted that in Fig. 1(c) the flavor indices in the quark loop are separately traced from those in the propagators associated with the nucleon interpolation field which reflect the valence nature of the proton. Hence, Fig. 1(c) does not distinguish a loop with the u quark from that with the d quark at the flavor symmetric limit, i.e. $m_u = m_d$. In other words, $u_s(x) = d_s(x)$. On the other hand, the origin of $u(x) \neq d(x)$ can come primarily from the antiflavor partons in Fig. 1(b). Thus, the violation of the Gottfried sum rule originates entirely from the cloud partons in the charge symmetric limit, i.e.

$$\int_0^Z dx \frac{F_2^p(x) - F_2^n(x)}{x} = \frac{1}{3} + \frac{2}{3} \int_0^Z dx [u_c(x) - d_c(x)]; \quad (7)$$

We shall see later that to $O(\alpha_s)$ and $O(1=Q^2)$, this turns out to be a sum rule.

3.3 Operator product expansion

In the Minkowski space, the operator product expansion (OPE) is carried out in the unphysical region of T which is defined with the time-ordered product of the currents. How does one carry this out in the Euclidean path-integral formulation? It turns out that because $\tilde{W}(q^2; \tau)$ is defined in the Euclidean path-integral (Eq. (2)), it requires several steps to get to T in the Minkowski space. On the other hand, it is relatively easy to do so because it involves a simple Taylor expansion of functions as opposed to dealing with operators in the usual OPE, as we shall see.

Considering Fig. 1(a) first, the three-point function in Eq. (2) involves the following expression

$$\tilde{W}(q^2; \tau) / \text{Tr} [\tilde{M}(t_1; t_2) \tilde{d}^3 x e^{iqx} i M^{-1}(t_2; t_1) i M^{-1}(t_2; 0)] ; \quad (8)$$

where M^{-1} 's are quark propagators with arguments labeled by the Euclidean time. The spatial indices are implicit and have been integrated over to give the nucleon a large momentum p and the momentum transfer q . x and τ are the spatial and time separations of the two currents J_1 and J_2 . The trace is over the color and spin indices. The expression in Eq. (8) gives the contribution from the quark line on which the currents are hooked. The other two quark propagators and the nucleon interpolation field operators are indicated by the dots.

Similar to the usual OPE derivation [10], we shall consider the most singular part of the quark propagator between the currents in Fig. 1. In the DIS limit where both the momentum transfer q^2 and energy transfer Q^2 are large, the leading singularity comes from the short-distance part in $\tilde{W}(q^2; \tau)$ where $q^2 \ll Q^2$ and $Q^2 \gg 0$. In this case, the

leading twists come from the short distance part. Therefore, we replace the quark propagator between the currents with the free massless propagator

$$M^{-1}(t_2; t_2) \rightarrow ! \frac{1}{4^2} \frac{\not{q}}{\not{x}^2 + \not{p}^2} : \quad (9)$$

We also carry out the Taylor expansion of the propagator $M^{-1}(t_2; 0)$ for small x

$$M^{-1}(t_2; 0) = e^{x \not{D} + \not{D}} M^{-1}(t_2; 0); \quad (10)$$

where D is the covariant derivative. With these substitutions, the corresponding hadronic tensor $W(q^2; \not{x})$ from Fig. 1(a) after the Fourier transform in space and Laplace transform in (Eq. (3)) is given as

$$W(q^2; \not{x}) / \text{Tr} [\not{M}(t; t_2) i \frac{i(\not{q} + i\not{\partial})}{\not{q} + i\not{D}} (+ D \not{x} + i\not{D}) i M^{-1}(t_2; 0)] : \quad (11)$$

Since $W(q^2; \not{x})$ is the imaginary part of T , i.e. $W(q^2; \not{x}) = \frac{1}{2} \text{Im } T(q^2; \not{x})$, one can use the dispersion relation to obtain T from W

$$T(q^2; \not{x}) = \frac{1}{Q^2 = 2M_N + D} \int_0^{\infty} \frac{W(q^2; \not{x})}{Q^2 + D^2} (+ D \not{x} + i\not{D}) i M^{-1}(t_2; 0); \quad (12)$$

where we have used $\not{x} = it$ and $D_t = i\not{D}$ so that $D = (\not{D}; i\not{D}_t)$ is the covariant derivative in Minkowski space. Expanding T in the unphysical region where $\frac{2p \cdot q}{Q^2} < 1$, the expression between the \not{x} 's in Eq. (12) gives

$$\frac{i(\not{q} + i\not{\partial})}{Q^2 + 2iq \not{D} + \not{D}^2} = \frac{i(\not{q} + i\not{\partial})}{Q^2} \sum_{n=0}^{\infty} \left(\frac{2iq \not{D} + \not{D}^2}{Q^2} \right)^n : \quad (13)$$

From this we obtain the valence and cloud parton leading twist contributions to T from Fig. 1(a)

$$T(q_{V+C}) = \sum_f e_f^2 \not{p} p \sum_{n=2}^{\infty} \frac{(-2q \not{p})^2}{(Q^2)^{n-1}} A_f^n (C : \not{x} :) - 2 \sum_{n=2}^{\infty} \frac{(-2q \not{p})}{(Q^2)^n} A_f^n (C : \not{x} :) + \dots \quad (14)$$

where f indicates flavor. The $A_f^n (C : \not{x} :)$ is defined through the following consideration. We first note that the short-distance expansion Eq. (13) leads the $T(q_{V+C})$ defined through the 4-point function in Fig. 1(a) to a series of terms represented by the three-point functions in Fig. 3(a) which correspond to matrix elements calculated through the C.I. expression

$$\text{Tr} [\not{M}(t; t_2) O_f^n M^{-1}(t_2; 0)] ; \quad (15)$$

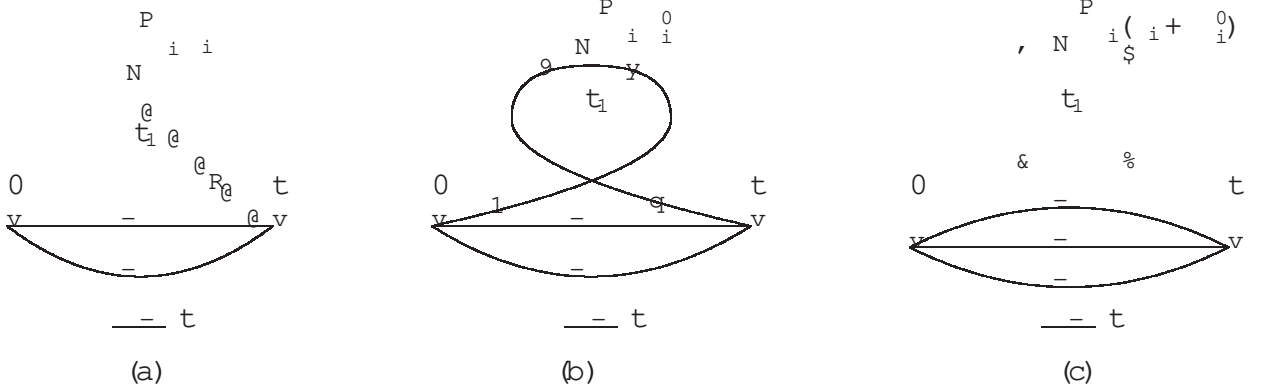


Figure 3: Quark skeleton diagrams in the Euclidean path integral formalism considered in the evaluation of matrix elements for the sum of local operators from the operator product expansion of $J(x)J(0)$. (a), (b) and (c) corresponds to the operator product expansion from Fig. 1 (a), 1 (b) and 1 (c) respectively.

where the operator O_f^n is

$$O_f^n = i \cdot 1 \left(\frac{i}{2}\right)^{n-1} \frac{\$}{D_2} \frac{\$}{D_3} \cdots \frac{\$}{D_n} : \quad (16)$$

The ratio of these three-point function in Fig. 3 (a) to the appropriate two-point functions then define the forward matrix element which in turn defines the coefficient $A_f^n(C:\!I:)$ in Eq.(14).

$$h p j O_f^n | p i_{C:\!I:} = A_f^n(C:\!I:) 2 p_1 p_2 \cdots p_n : \quad (17)$$

Similarly, we can perform the short-distance expansion for the anticloud parton in Fig. 1 (b) and obtain the same expression as in Eq. (14) except with the substitution $q \rightarrow -q$. As a result, this leads to the even n term sum minus the odd n terms instead of the sum as in Eq. (14), i.e.

$$T(C) = \sum_{\text{even}=2}^{\infty} \frac{n}{f} C:\!I: - \sum_{\text{odd}=3}^{\infty} \frac{n}{f} C:\!I: \quad (18)$$

In other words, the short-distance expansion of T in Fig. 1 (b) gives the three-point functions with a series of insertion of the same operators O_f^n except with a minus sign for the odd n terms. This is illustrated in Fig. 3 (b) where $\frac{0}{n}$ denotes the n -th

term insertion with the operator O_f^n and the associated kinematic factors in Eq. (??). Comparing 0_n in Fig. 3(b) the corresponding n_n in Fig. 3(a), the minus sign for the odd n terms in Eq. (18) implies that ${}^0_n = (-)^n {}^n_n$.

By the same token, the short-distance expansion for the quark/antiquark propagator of T from Fig. 1(c) gives

$$T(q_s = \bar{q}_s) = \sum_{\text{even } n=2}^X A_f^n (D \cdot I) : \quad \sum_{\text{odd } n=3}^X A_f^n (D \cdot I) : \quad (19)$$

They have the same expression as $T(v + c)$ and $T(q_s)$ except $A_f^n (D \cdot I)$ are from the D . I. part of the matrix element

$$h p j O_f^n \not{p} D \cdot I = A_f^n (D \cdot I) 2 p_1 p_2 \cdots p_n : \quad (20)$$

In this case, the leading twist expansion of the sea contribution to T in Fig. 1(c) now leads to two series of forward matrix elements of D . I. One is for $T(q_s)$ with even plus odd n terms; the other is $T(q_s)$ with even minus odd n terms as given in Eq. (19). Both are represented in the three-point functions in Fig. 3(c).

When the parts in Eqs. (14), (18), and (19) are summed up, only the even n terms of the OPE are left

$$\begin{aligned} T &= T(q_{s+c}) + T(q_s) + T(q_s + \bar{q}_s) \\ &= 2 \sum_{n=2, \text{even}}^X (A_f^n (C \cdot I) + A_f^n (D \cdot I)) : \end{aligned} \quad (21)$$

This is the same as derived from the ordinary OPE. However, what is achieved with the path-integral formulation is the separation of C . I. from D . I. in addition to the separation of partons from antipartons which has not been possible with other formulation, e. g. light-cone definition of the distribution function. This separation facilitates the derivation of the different small x behavior between the C . I. and the D . I., the identification of the cloud parton, and a different evolution of $q_c(x; Q^2)$ from that of $q_s(x; Q^2)$ and $\bar{q}_s(x; Q^2)$ as we shall see.

Now consider the contour integral of T_2 in the C . I. and D . I. parts of T around $= 0$ in the complex plane while keeping Q^2 fixed. $\frac{1}{2} \int \frac{d}{2i} \frac{T_2(\not{Q}^2)}{n-1}$ picks up the $n=2$ term in the series expansion of T_2 in Eqs. (14), (18), and (19) (N.B. $2q \cdot p = 2M_p$ in these equations.)

$$\frac{1}{2} \int \frac{d}{2i} \frac{2M_p}{n-1} T_2(\not{Q}^2) = \sum_f^X 8e_f^2 \left(\frac{2M_p}{Q^2} \right)^{n-1} A_f^n : \quad (22)$$

for both the C . I. and the D . I. The contour of the integral can be distorted to turn the above integral into an integral over the discontinuities of T_2 through the dispersion relation

$$2 \int_{Q^2}^{Z-1} \frac{d}{2i} \frac{2M_p}{n-1} 2i \text{Im} T_2(\not{Q}^2) = 8 \left(\frac{2M_p}{Q^2} \right)^{n-1} \int_0^{Z-1} dx x^{n-2} \frac{2M_p}{4} W_2(\not{Q}^2) : \quad (23)$$

Equating these two integrals and relating W_2 to the parton distribution function, we can obtain the moment sum rules. Since $T_2(Q^2)$ is symmetric w.r.t. τ , we obtain only the sum rules for even n . Thus we obtain

$$\begin{aligned} A_f^{n=\text{even}}(C : I:) &= M^{n-1}(C : I:) \int_0^{Z_1} x^{n-1} (q_{V+c}(x; Q^2) + q_F(x; Q^2)); \\ A_f^{n=\text{even}}(D : I:) &= M^{n-1}(D : I:) \int_0^{Z_1} x^{n-1} (q_S(x; Q^2) + q_B(x; Q^2)); \end{aligned} \quad (24)$$

Similarly we obtain the moment sum rules for the odd n from the W_3 form factor through the interference of the vector and axial vector currents

$$\begin{aligned} A_f^{n=\text{odd}}(C : I:) &= M^{n-1}(C : I:) \int_0^{Z_1} x^{n-1} (q_{V+c}(x; Q^2) - q_F(x; Q^2)); \\ A_f^{n=\text{odd}}(D : I:) &= M^{n-1}(D : I:) \int_0^{Z_1} x^{n-1} (q_S(x; Q^2) - q_B(x; Q^2)); \end{aligned} \quad (25)$$

One can define the valence parton distribution

$$q_V(x; Q^2) = q_{V+c}(x; Q^2) - q_F(x; Q^2); \quad (26)$$

In this case, $A_f^{n=\text{odd}}$ gives the sum rule for the valence distribution. In particular, valence number sum rules

$$\begin{aligned} M_u^0(C : I:) &= \int_0^{Z_1} dx u_V(x; Q^2) = 2; \\ M_d^0(C : I:) &= \int_0^{Z_1} dx d_V(x; Q^2) = 1; \\ M_f^0(D : I:) &= \int_0^{Z_1} dx (q_S(x; Q^2) - q_B(x; Q^2)) = 0; \end{aligned} \quad (27)$$

for the u and d quarks in the proton reflect the charge conservation of the vector current i_V and that the sea carries no net charge.

We note that the matrix elements associated with $A_f^{n=\text{even}}(C : I:)$ include not just the valence but also the cloud contribution. This is why the matrix element $A_{u,d}^2(C : I:)$ which corresponds to the $M^1(C : I:) = hxi_{C,I:}$ when calculated on the lattice [11, 12] are larger than those obtained from the experiments for the valence partons only, i.e. hxi_V .

3.4 Operator Rescaling and Matching, and Parton Evolution

The dimensionless coefficients A_f^n are not constants, but depend logarithmically on Q^2 , the renormalization point of the operator product expansion. The operator rescaling and matching analysis [13, 14] for the twist-two flavor non-singlet and singlet operators gives the renormalization group equations for the corresponding moments of the

structure functions. In the context of the present path-integral formulation of OPE, the non-singlet coefficients A_f^n and the non-singlet moments only have contributions from the C. I. (Fig. 3(a) or Fig. 3(b)), since their D. I. contributions cancel among the different avors. On the other hand, the singlet coefficients A_f^n and the singlet moments have both the C. I. and D. I. (Fig. 3(c)) contributions. Therefore, it is possible to go to the single avor basis and classify the equations in terms of C. I. and D. I. For the C. I. which involves only the valence avors (e. g. u and d for the nucleon), the renormalization equation is

$$\frac{d}{d \ln Q^2} M_f^n (C: \square:) = \frac{s(Q^2)}{8} a_{qq}^n M_f^n (C: \square:); \quad (28)$$

where a_{qq}^n is the anomalous dimension coefficient. For the D. I. the equation is

$$\frac{d}{d \ln Q^2} M_f^n (D: \square:) = \frac{s(Q^2)}{8} (a_{qq}^n M_f^n (D: \square:) + \frac{1 + (-)^n}{2} a_{qG}^n M_G^n); \quad (29)$$

where a_{qG}^n is the anomalous dimension coefficient for operator mixing with the gluon operators and M_G^n is the moment for the gluon distribution function. We note that this mixing with gluon operators only contribute to $n = \text{even}$. As we see this equation involves the sea parton only, i. e. u_s, d_s ; and s .

We should stress that in the literature [15, 17, 18] the non-singlet has been identified with valence. This is clearly incorrect. As we see from Eq. (24) that $A_f^{n=\text{even}} (C: \square:)$ includes the cloud partons in addition to the valence. Detailed study of this subject on the lattice has been carried out for thematrix elements and form factors of the nucleon from the three-point functions and hadron masses from the two-point functions [4]. It is shown when the cloud quarks are removed by prohibiting pair-production through the Z graphs in the C. I., the hadron structure and masses are greatly affected. It is learned that the cloud quarks are responsible for the meson dominance in the form factors, the deviation of $F_A = D_A$ and $F_S = D_S$ from the non-relativistic $SU(6)$ limit, the hyperfine splittings, and the constituent quark masses. In the context of the parton model, they are responsible for the difference of $u(x)$ and $d(x)$ in the proton.

Following Atarelli and Parisi [15], the rescaling and mixing equations in Eqs. (28) and (29) can be translated into integral-differential equations which are the evolution equations for the parton densities. Therefore, for the C. I. the evolution equation for the unpolarized valence and cloud parton is

$$\frac{d q_{V+c}(x; Q^2)}{d \ln Q^2} = \frac{s(Q^2)}{2} \int_x^{z=1} \frac{dy}{y} P_{qq} \left(\frac{x}{y} \right) q_{V+c}(y; Q^2); \quad (30)$$

where

$$\int_0^{z=1} dz z^{n-1} P_{qq}(z) = \frac{a_{qq}^n}{4}; \quad (31)$$

For the anticloud parton density, the equation is similar

$$\frac{d q_c(x; Q^2)}{d \ln Q^2} = \frac{s(Q^2)}{2} \int_x^1 \frac{dy}{y} P_{qq} \left(\frac{x}{y} \right) q_c(y; Q^2); \quad (32)$$

For the sea-partons in the D. I. (Fig. 1(c)), the evolution equations from Eq. (29) are

$$\begin{aligned} \frac{d (q_s + q_{\bar{s}})(x; Q^2)}{d \ln Q^2} &= \frac{s(Q^2)}{2} \int_x^1 \frac{dy}{y} P_{qq} \left(\frac{x}{y} \right) (q_s + q_{\bar{s}})(y; Q^2) + P_{qG} \left(\frac{x}{y} \right) G(y; Q^2); \\ \frac{d (q_s - q_{\bar{s}})(x; Q^2)}{d \ln Q^2} &= \frac{s(Q^2)}{2} \int_x^1 \frac{dy}{y} P_{qq} \left(\frac{x}{y} \right) (q_s - q_{\bar{s}})(y; Q^2); \end{aligned} \quad (33)$$

where

$$\int_0^1 dz z^{n-1} P_{qG}(z) = \frac{a_{qG}^n}{4}; \quad (34)$$

and $G(y; Q^2)$ is the unpolarized gluon distribution function.

Finally, the gluon evolution equation is

$$\begin{aligned} \frac{d G(x; Q^2)}{d \ln Q^2} &= \frac{s(Q^2)}{2} \int_x^1 \frac{dy}{y} P_{Gq} \left(\frac{x}{y} \right) \left[\sum_{f=\text{val:fla:}}^x (q_s^f + q_{\bar{s}}^f) + \sum_{f=\text{sea:fla:}}^x (q_s^f - q_{\bar{s}}^f) \right] (y; Q^2) \\ &+ P_{GG} \left(\frac{x}{y} \right) G(y; Q^2); \end{aligned} \quad (35)$$

We see that the equations for the gluon and the sea distributions are the same as others in the literature [18, 17, 20]. Yet, there is an extra cloud degree of freedom in the evolution of the non-singlet parts (Eqs. (30) and (32)). This part has not been incorporated in the dynamical degrees of freedom in the parton model, as far as we know. It can not be simply accommodated in Eq. (33) since it has a different small x behavior than the sea as alluded to earlier.

Due to the fact that

$$\int_0^1 dx P_{qq}(x) = \frac{a_{qq}^1}{4} = 0; \quad (36)$$

we have

$$\frac{d}{d \ln Q^2} \int_0^1 dx q_v(x; Q^2) = 0; \quad (37)$$

$$\frac{d}{d \ln Q^2} \int_0^1 dx q_c(x; Q^2) = 0; \quad (38)$$

We see that the cloud antiparton number, like the valence number, is conserved. This is in contrast with the sea whose number is not conserved due to the pair-creation from the gluon. However, the conservation of the cloud number is only good in the

leading logarithm is approximation. Whereas, the conservation of the vector current protects the charges against any Q^2 correction [13, 14, 15].

We note that the sum in Eq. (7) is in terms of the cloud antipartons numbers. Thus to leading logarithm is approximation, it is a sum rule

$$\int_0^z \frac{dx}{x} \frac{F_2^p(x) - F_2^n(x)}{x} = \frac{1}{3} + \frac{2}{3} [n_{u_c} - n_{d_c}]; \quad (39)$$

where $n_{u_c} = n_{d_c}$ is the $u_c = d_c$ number.

3.5 Magnitude of the cloud and anticloud partons

We don't know how large the cloud and anticloud partons are in comparison with the valence and the sea unless one fits the DIS and Drell-Yan experiments with an explicit separation of the cloud and the sea. But there are hints which are helpful in this respect. From the NMC experiments on the F_2 structure function of the proton and deuteron [2], the sum rule in Eq. (39) is measured to be 0.235 - 0.026, significantly smaller than the Gottfried prediction of 0.333. This implies that

$$n_{u_c} - n_{d_c} = \int_0^z dx [u_c - d_c] = 0.147 - 0.039; \quad (40)$$

at $Q^2 = 4 \text{ GeV}^2$ which is not negligible compared with the valence numbers of u and d .

Since u (similarly for d) have contributions from the cloud and the sea, i. e. $u(x) = u_c(x) + u_s$ and s is from the sea only, one expects that

$$hxi_u = hxi_{u_c} + hxi_{u_s} > hxi_s: \quad (41)$$

Indeed, in the CTEQ 4 analysis [19] one finds that $\frac{1}{2} (hxi_u + hxi_d) = 2hxi_s$ at $Q_0 = 1.6 \text{ GeV}$. At very small x , i. e. 10^{-4} , $u=d$ is dominated by $u_s=d_s$. Therefore, $u=d$ is in this range. The recent global analysis of the parton structure (CTEQ 5) [20] shows that $u = d = 1.05 s$ in this small x range. Assuming that the functional form of the sea parton distribution does not depend on the sea-quark mass, we then conclude

$$\frac{1}{2} (hxi_{u_s} + hxi_{d_s}) = 1.05 hxi_s: \quad (42)$$

It then implies that at $Q_0 = 1.6 \text{ GeV}$

$$\frac{1}{2} (hxi_{u_c} + hxi_{d_c}) = \frac{1}{2} (hxi_{u_s} + hxi_{d_s}): \quad (43)$$

In other words, the momentum fraction of $u+d$ is about evenly divided into the cloud and sea contributions at $Q_0 = 1.6 \text{ GeV}$.

4 Conclusion

In conclusion, we have formulated the hadronic tensor W of the deep inelastic scattering starting from the Euclidean path-integral formalism. We found that it can be divided into three gauge-invariant and topologically distinct parts which we classify as the valence-cloud, the anticloud and the sea. This allows a separation of the C. I. from the D. I. and the partons from the antipartons. Since the cloud is in the C. I. and the sea in the D. I., they have very different small x behavior. We show that the operator product expansion is simply a Taylor expansion of short distance in the path-integral. From operator rescaling and mixing, we derive the evolution equation which shows that the cloud and anticloud partons evolve like the valence and their numbers are conserved in the leading log approximation. In view of the fact that at small x , $q^2 / x^{1/2}$ which is different from the sea, a reanalysis of the global experimental data with explicit separation of the cloud and the sea is necessary. This will lead to a different quark and gluon parton distribution functions from those of the present fits at large Q^2 .

This work is partially supported by U.S. DOE grant No. DE-FG 05-84ER 40154. The author would like to thank S. Brodsky, N. Christ, G. T. Garvey, X. Ji, L. Mankiewicz, R. M. Cahn, C. S. Lam, G. Martinelli, J. C. Peng, and C. P. Yuan for useful discussions.

References

- [1] J. Ashman et al. (EMC), *Phys. Lett. B* 206, 364 (1988); K. Abe et al. (E143), *Phys. Rev. Lett.* 74, 346 (1995); D. Adams et al. (SMC), *Phys. Rev. D* 56, 5330 (1997).
- [2] NMC Collaboration, P. Amoudru et al., *Phys. Rev. Lett.* 66, 2717 (1992); M. Amendo et al., *Phys. Rev. D* 50, R1 (1994).
- [3] K. F. Liu and S. J. Dong, *Phys. Rev. Lett.*, 72, 1790 (1994).
- [4] K. F. Liu, S. J. Dong, T. D. Raper, D. Leinweber, J. Sloan, W. Wilcox, and R. M. Woloshyn, *Phys. Rev. D* 59, 112001 (1999).
- [5] W. Wilcox, *Nucl. Phys. (Proc. Suppl.)*, B 30, 491 (1993).
- [6] This point was brought up by R. Jaffe during the Gordon Conference on Nuclear Physics and QCD in July 1999.
- [7] See, for example, S. Adler and R. Dashen, *Current Algebra and Applications to Particle Physics*, pp. 254 (Benjamin, N.Y., 1968).

[8] S. B rodsky and I. Schmidt, Phys. Rev. D 43, 179 (1991).

[9] E 866/NuSea Collaboration, J. C. Peng et al., Phys. Rev. D 58, 092004 (1998).

[10] We shall follow the derivation of operator analysis in M. E. Peskin and D. V. Schroeder, Quantum Field Theory, Addison-Wesley, 1995.

[11] G. Martinelli and C. T. Sachrajda, Nucl. Phys. B 316, 355 (1989).

[12] M. Gockeler, et al., Phys. Rev. D 53, 2317 (1996).

[13] H. Georgi and H. D. Politzer, Phys. Rev. D 9, 416 (1974).

[14] D. Gross and F. Wilczek, Phys. Rev. D 9, 980 (1974).

[15] G. Altarelli and G. Parisi, Nucl. Phys. B 126, 298 (1977).

[16] L. N. Lipatov, Yad. Fiz. 20, 181 (1974) [Sov. J. Nucl. Phys. 20, 94 (1975)].

[17] J. C. Collins and J. Qiu, Phys. Rev. D 39, 1398 (1989).

[18] E. Eichten, et al., Rev. Mod. Phys. 56, 579 (1984).

[19] H. L. Lai, et al., Phys. Rev. D 55, 280 (1997).

[20] H. L. Lai, et al., hep-ph/9903282.